Fuel 351 (2023) 128907

Contents lists available at ScienceDirect

Fuel

journal homepage: www.elsevier.com/locate/fuel

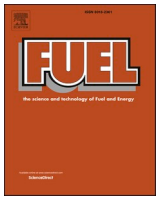

Full Length Article

Effect of air staging and porous inert material on the emission of volatile organic compounds in solid biomass combustion

Juan Jesús Rico *, Raquel Pérez-Orozco, Jacobo Porteiro, David Patiño

CINTECX, University of Vigo, Lagoas-Marcosende, s/n, Vigo, Pontevedra 36310, Spain

ARTICLE INFO

Keywords:
Biomass
Combustion
Volatile organic compounds
Porous inert material
Thermogravimetric analysis

ABSTRACT

The present paper delves into experimental data to assess the effects of the inclusion of a zirconium porous medium in the emissions of a laboratory-scale biomass combustor, with a focus on particulate matter and volatile organic compounds. While other studies have focused on the effects of the material on solid particulate matter or gaseous emissions, this research is focused on volatiles, their capture and storage. A novel sampling train for the capture of volatiles has been designed based on active carbon adsorption on a refrigerated environment, and its performance was evaluated through thermogravimetric analysis, showing the affinity of this porous medium towards lighter organic compounds. The retention time of the sample was also studied, and the data revealed that after three to six hours the sample had degraded significantly when stored in airtight plastic bags inside a glass desiccator at 22 °C. An analysis of the particulate matter emitted was also carried out. Volatile organic compounds were also found to follow the behavior of particulate matter, with the scenarios where low solid particles were emitted being also those in which volatiles release was minimized.

1. Introduction

The ever changing social and political landscape has, in the last few decades, followed an accelerating trend towards the adoption of more renewable power in the energy grids. Events as the COVID-19 pandemic or the war in Ukraine have put the European Union's energy systems to a test and implementing green and sustainable alternatives to fossil fuels has become crucial to substitute the missing energy sources and ensure a lower energy dependency on third countries [1–5]. Furthermore, the effects of climate change are becoming impossible to ignore, with hotter, dryer summers and more recurrent extreme weather events of a magnitude not witnessed before [6–8]. In this scenario, policymakers and the general public alike have as one of their paramount interests to support and enforce ever stricter regulations concerning environmental pollution, energy efficiency, generation of renewable power and the promotion of sustainable development.

Volatile organic compounds (VOCs) comprise a wide array of substances, ranging from small molecules such as pentanes or benzene up in their number of carbon atoms until larger sized ones such as mono- or sesquiterpenes [9]. In the field of biomass, they all have in common their low evaporation temperatures, some are in a gaseous form at room temperature, while others stay in liquid form up to 200 °C [10]. These compounds are known for playing a role in the formation of tropospheric ozone when interacting with nitrogen oxides and carbon monoxide in presence of sunlight [11,12]. Not only that, but VOCs also pose a non-negligible health risk for humans, especially in cases of high concentration indoors, where allergic or even immune reactions are known to be more frequent. Given the high variety of compounds that are considered VOCs, their health effects can vary from negligible to high toxicity, depending also on the exposure levels and time [13–15]. Furthermore, VOCs are a source of particulate matter (PM) emissions, as the existence of links between the two substances has been suggested by research performed in the last decade [16–18]. Photochemical oxidation of VOCs such as isoprene has been related to PM contamination mainly in rural areas [19], while other studies suggest that up to a 2.4 % of PM2.5 could have its origin in VOCs in urban environments [20].

Given their diversity, the capture and analysis of VOCs is a remarkably difficult process requiring absorption in organic substances [21,22] or the utilization of low temperature methods combined with highly specialized substrates for the adsorption of such organic compounds. Such substrates have a high affinity for some specific compounds, while not adsorbing others, or doing it poorly, which leads to misrepresentation of some compounds in favor of others. The clearest example of this behavior is Active Carbon (AC), an inexpensive substrate that can be

* Corresponding author.
E-mail address: jjrico@uvigo.gal (J.J. Rico).

https://doi.org/10.1016/j.fuel.2023.128907
Received 1 March 2023; Received in revised form 19 May 2023; Accepted 3 June 2023
Available online 11 June 2023

either commercially supplied or produced on-site from vegetal residues. The large specific surface of AC and its rich pore structure make it a common choice for gas purification, especially in the field of VOC treatment [23,24]. Past studies have found that the pores generally present in such a material have a great affinity to monocyclic aromatic hydrocarbons and aldehydes, among other organic substances [25–28], and low-temperature capture is also developed as a means to improve the adsorption rate of the substances [29]. One of the main challenges found, besides the obvious implications of the selectivity of the AC in VOC capture, is the irregularity of the pores of the material, that difficult the task of proposing a clear-cut affinity for the material, although some efforts have succeeded in creating semi-homogeneous mesopores of a predetermined size via specific treatments [30,31].

In biomass combustion, one of the main issues regarding pollution is particulate matter (PM). These pollutants can be significantly threatening to human health due to their small diameter, as in biomass combustion the predominant size of PM is under 1 μm (PM_1), although the size distribution has been found, in some cases, to be bimodal, with a secondary peak around 2–10 μm [32]. To reduce PM pollution, one of the most effective strategies is to establish an air-staging procedure, consisting in splitting the air inlet into a primary inlet under the combustion bed and a secondary inlet a set distance above the bed. This technique allows for a better air–fuel mixture and is sometimes reinforced with a tertiary air inlet to further improve the combustion [33,34]. As temperatures reached within the combustion chamber are lower than in liquid and gaseous fossil fuels, thermal nitrogen oxides pose a lesser threat in woody biomasses, nevertheless the high nitrogen content of the fuels compensates this effect, making NOx a main issue in the gaseous emissions from biomass combustion. In non-woody or residue-derived fuels their presence is significantly higher than in commercial wood pellets [35,36].

In the field of biomass, a novel strategy that has proven to be effective in controlling emissions is the inclusion of a porous inert material (PIM) in the upper stages of the gas flow after the combustion chamber and the secondary air inlet [37]. While still in the early stages of its development and implementation in real facilities, the research proposes that this material, usually a ceramic resistant to extreme temperature gradients, acts as an optical barrier that confines the flame, increasing temperature in the combustion chamber and leading to improved reactions in the volume beneath it, and results indicate reductions in PM emissions when the optimal conditions are achieved. The most relevant parameter for reaching these conditions seems to be the positioning of the material, as its influx on the air flow and combustion conditions are more noticeable the closer it is to the combustion chamber, while placing it too far away negates its positive effects [38,39].

In this paper, a study on the effects of the combination of both strategies mentioned previously, air staging and PIM inclusion, is performed. A simplified active carbon-based VOC sampling system is proposed, that is used for the analysis of emitted VOCs in an experimental solid biomass combustion facility, where the main variables are the introduction of air in different proportions in two stages of the combustion chamber and the presence or absence of a porous inert material at a fixed point of the facility. Thermogravimetric analyses (TGA) are carried out to assess the extent of the variations on VOCs captured by the proposed methodology. The main novelties of this research reside on the one hand in the design and testing of a novel VOC capture system and, on the other hand, in the combined analysis of the consequences of inserting a porous inert material on PM and VOC emissions.

2. Materials and methods

2.1. Biomass fuel

A commercial wood pellet of the standard of quality ENplus A1, determined by the European standard EN 16127, was used for the tests performed in the facility. The relative stability of its composition has been proven over the years, with its proximate and ultimate analysis, as well as its heating value, diverging by a slight margin in the analyses performed and reported in previous works [40–42]. This allows for easier repeatability of results with other studies performed in this research group, as well as for direct comparison with other studies in the field. In the Supplementary Material, Table A1 gathers the most relevant data of the fuel and its properties. As is characteristic for most commercial wood pellets, levels of moisture and ash are low, therefore heating value will reach levels close to the ideal maximum values reported in literature for this feedstock [43–45]. Ash content was determined following EN ISO 18122:2016, while ultimate analysis was carried out following EN ISO 16948:2015 and EN ISO 16994:2017. Heating values were calculated by following the procedure dictated in EN ISO 18125:2018.

2.2. Test facility

The facility in which the experiments have been performed is a lab-scale custom biomass burner equipped with state-of-the-art sensors and regulation devices, that allow for a precise and thorough control of the inputs and outputs of the installation. It can be seen in Fig. 1.

The main body of the facility is built in 316L stainless steel, it possesses an overfed combustion chamber and a two-stage air inlet, with primary air under the chamber, 100 mm below the grate, and secondary 150 mm over it. The facility is completely modular, allowing for the addition or removal of sections depending on the intended use or the technology evaluated. For this case scenario, a slim porous inert material holder was designed and incorporated, causing minimal disturbances to the overall facility, and allowing for the results obtained to be compared to those without PIM module.

The facility has a square cross section with an interior surface of 225 cm^2. The grate of the combustion chamber is flat, and the PIM is located 40 cm above it.

Two refrigeration circuits can be utilized while testing, cooling the combustion chamber and the main frame of the facility independently, and in this research both systems were in use. These refrigeration systems release heat thanks to a forced convection dissipation system consisting in two independent heat exchange systems sized in

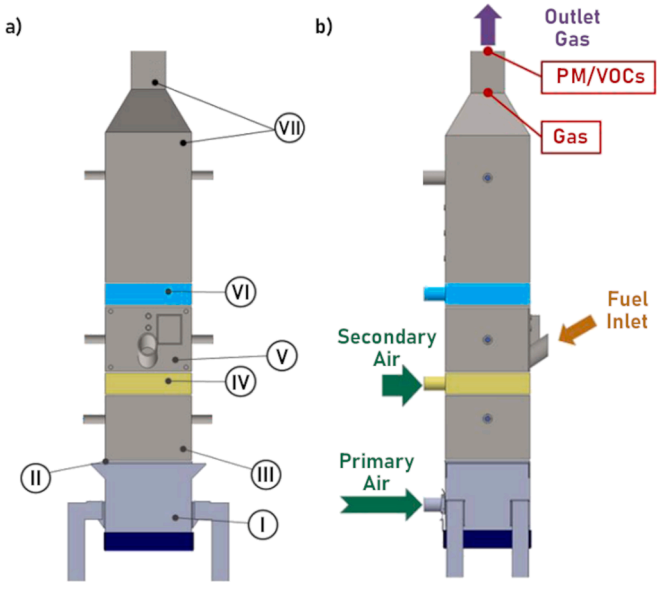

Fig. 1. View of the experimental facility. a) Module disposition, I. Plenum, II. Grate, III. Combustion bed, IV. Secondary air, V. Combustion chamber, VI. PIM holder, VII. Post-combustion chamber; b) Inlets (with arrows) and sampling ports (encircled).

accordance with the design flow rate of water of each cooling circuit.

Data gathered by the sensors and inputs given to the actuators are centralized in a computerized acquisition system every second, and results are stored for further processing.

Results regarding prior configurations and a more thorough description of the facility and its capabilities can be found in previous literature, as well as the base work with PIM performed in the predecessor of the current biomass burner that initiated the research conducted here [37,46,47].

2.3. Porous inert material

A zirconium oxide-based ceramic foam (Manguitos Arrosi, Spain) was installed in some of the tests performed in the facility. This foam is a common industrial material, utilized in blast furnaces to filter molten metal and remove the oxides formed in the surfaces in contact with air. It is thus a material highly resistant to sharp temperature changes and known for being inert to most chemicals. Withstanding temperatures up to 1750 °C and with a high porosity, this material confines heat in the areas below it while not altering the gas flow. As it has been observed in previous research the pressure drop caused by the PIM is negligible for a single layer of ceramic [37]. The material is chosen for its excellent thermal capabilities, resistance to thermal shock and pronounced thermal gradients and mechanical durability. It is also a common material in metallurgy industries given its relatively affordable price, therefore its use is also due to its availability. It is preferred to other similar materials such as silicon carbide (SiC) or aluminum oxide (Al_2O_3) given its higher thermal resistance of up to 1750 °C, compared to the 1550 °C of SiC and 1100 °C of Al_2O_3, according to the manufacturer.

A square slab of 150 × 150 mm and a porosity of 10 pores per inch (ppi) was placed inside a holder designed to blend in with the rest of the facility, as seen in Fig. 2, and positioned 300 mm above the base of the combustion bed, above the secondary air inlet without obstructing it.

2.4. Measurement devices

2.4.1. Temperature measurement

The facility incorporates several ports for the inclusion of 6 mm K-type thermocouples. Nine of them are situated in the combustion chamber, forming a 3 × 3 array aiming to register temperatures in the center plane of the chamber. Four more thermocouples are located in the post-combustion chamber, and a further one on the chimney, to gather data on the evolution of flue gas temperature. The names and position of the thermocouples can be observed in Table 1, while their location is presented in Fig. 3.

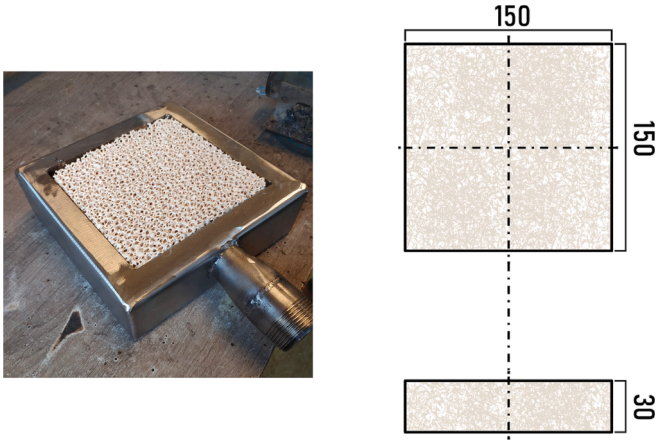

Fig. 2. Porous inert material inside its module (left) and dimensions in mm (right).

Table 1
Thermocouples in the facility. Dimensions in mm measured from the grate.

Thermocouple	ID	Position (mm)
Combustion chamber bottom	TBT	12
Combustion chamber middle	TMD	50
Combustion chamber top	TUP	95
Porous Inert Material	TPIM	300
Post combustion chamber bottom	TP1	430
Post combustion chamber middle	TP2	480
Post combustion chamber top	TP3	530
Chimney	TCH	1460

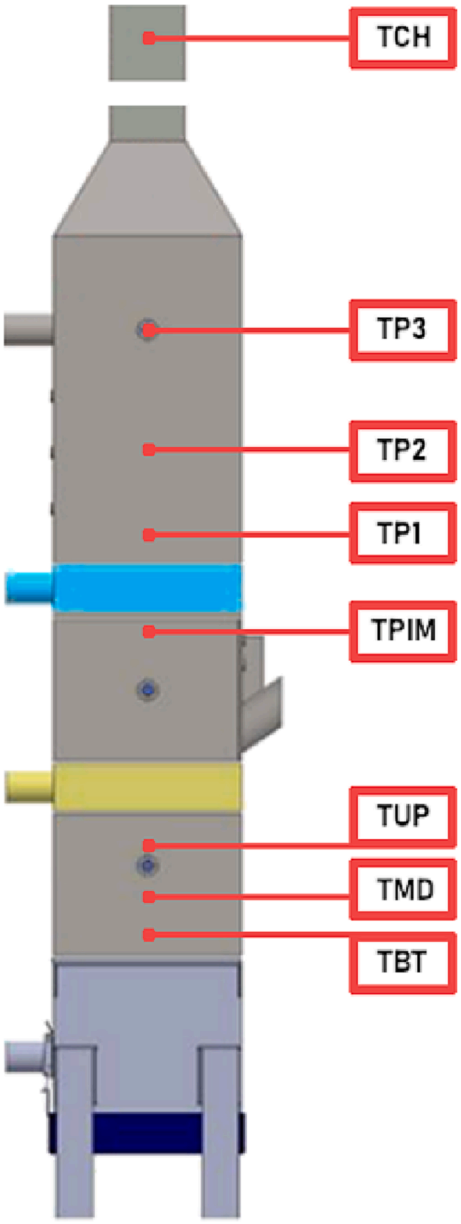

Fig. 3. Position of thermocouples in the facility.

2.4.2. Gas analyzer

A Servomex 4900 (Servomex, United Kingdom) was used to analyze a sample of flue gas and determine the proportion of oxygen, carbon monoxide and nitrogen oxides. The gas sample was prefiltered at the facility and transported through a heated conduction at 120 °C towards a scrubbing station, in which moisture is removed from the stream by

rapidly lowering its temperature to the dew point. A second filtering is performed to eliminate the finer solid particles. This device records gas composition every second, and the data is integrated in a database that also records temperatures, flow rates, and fuel levels.

2.4.3. TGA-DTA/Dsc

Thermogravimetric analyses were carried out in a TGA-DTA/DSC Setaram Labsys system (KEP Technologies, France). The characteristics of the apparatus as used for the experiments leading to this research are listed in the Supplementary Material's Table A2. The TGA was used for the desorption of organic species from the AC, with the lighter compounds desorbing at lower temperatures than the heavier ones. Besides, a study on sample degradation was performed by completing the desorption at different times after adsorption and storage.

2.5. VOC sampling train

Volatile organic compounds are, by their diverse nature, difficult to capture and retain. The lightest species evaporate at around 50 °C, while the heaviest ones could stay liquid up until 250 °C, and the variety of molecule sizes and morphologies, functional groups and affinities towards certain substrates makes designing a simple, portable, and effective adsorption system a real challenge. The use of active carbon as adsorbent media is widely reported in literature to be effective in a wide range of chemical species regardless of its origin or shape [23,48–50], and therefore it has been used in the tests reported in this research.

Two sealed glass impingers filled with a fixed mass of 60 g of active carbon pellets comprise the two adsorption cartridges. The first of them is at room temperature, while the second is partially submerged in propylene glycol to lower its temperature to − 20 °C, creating a pronounced temperature gradient that favors the condensation of volatiles over the AC surface. The two impingers are preceded by a silica gel-filled impinger intended to remove any moisture present in the gas flow, given that the high hygroscopicity of the active carbon could hamper the measurements as water fills the pores, rendering them unusable for the capture of volatile compounds. This three impingers comprise what is called the impinger train. The inlet rod of the impingers ends in a fritted glass section permeable to gas, guaranteeing a high turbulence in the gas flow entering each one of them, improving the contact between organic substances in the gas and the highly porous surface of the AC.

Before the impinger train the sampling device consists in an isokinetic probe inserted in the experimental facility followed by heated conductions delivering the sampled gas to a PM trap. The trap comprises an aluminum cylindric container holding a PTFE filter with a pore size of 0.3 μm. The container is also heated over the boiling point of water to prevent condensation related issues. The sample is then delivered to the impinger train.

After the impingers a second moisture trap is located as a standard protective measure for the pump, the flow rate of which is regulated through the use of a calibrated orifice. In this case, this orifice is designed to offer a flow rate of 16 lpm when the speed of the flow is sufficiently high, information that can be derived from the pressure drop occurring at the orifice, measured thanks to the manometers present at both entrance and exit. The schematics of this sampling train can be observed in Fig. 4.

2.6. Experimental methodology

A batch of twelve tests was carried out, consisting in two configurations of the facility: with and without PIM; and two air-staging strategies for each configuration: 30 % primary air and 50 % primary air. The corresponding nomenclature is shown in Table 2, and the general parameters of the facility are briefly stated in Supplementary Material's Table A3. Each test was performed thrice to ensure reproducibility of the results. During each test, the first 45 min of combustion are considered to correspond to transitory regime, as temperatures and gas composition vary significantly in short spans of time. After stationary regime is reached and 10 min have passed, the impinger train is connected and allowed to collect VOC sample for 45 min.

As for VOC samples, time is of the utmost importance when handling the samples, to avoid the loss of mass during storage. The mass difference of the sealed glass containers is measured in situ, and a sample of active carbon is taken from each impinger to further process. The capture of VOCs with AC is well attested in literature, but nevertheless a thermal cycle in a TGA-DTA/DSC apparatus was performed to assess the volatilization point of the substances gathered and seek confirmation of their VOC nature. Thus, a heating cycle that can be observed in Supplementary Material's Figure A1 was applied to a sample of the AC used in the tests immediately after the tests were finished. Not only that, but

Table 2
Test nomenclature.

	Base tests	PIM tests
30% Primary Air	Base 30/70	PIM 30/70
50% Primary Air	Base 50/50	PIM 50/50

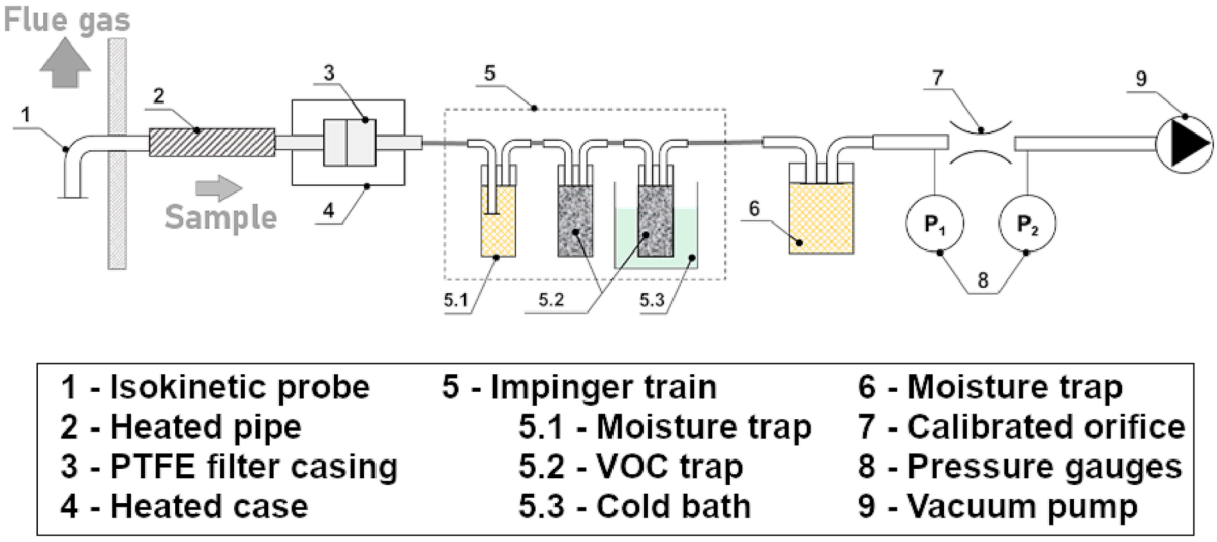

Fig. 4. Volatile organic compounds sampling train.

the same cycle was applied to AC samples at different times after their utilization to collect VOCs, to understand the effect of time and prolonged storage on the retention of the captured chemicals. With this intent, tests at 3, 6, 24, 48 and 72 h were performed. The storage of the AC after sample collection was inside airtight bags inside a desiccator at room temperature, therefore ensuring minimal moisture contamination.

3. Results and discussion

3.1. General performance

The first series of tests analyzed were the 30 % primary, 70 % secondary air, as they more closely resemble the conditions tested in previous facilities in the laboratory. As it can be seen in Fig. 5, temperatures in Base tests (without PIM) evolved as expected, with higher values in the combustion chamber and a steady decline the further away from the chamber each thermocouple is. The sudden drop in temperature happening at the second thermocouple in every test is interpreted as the sensor recording the temperature of the fresh fuel as it reaches the combustion chamber. A relevant selection of these results is numerically represented in Table 3. A typical profile of instabilities is also detected, with values oscillating up to a 10 % even when the represented times correspond to the stationary phase of combustion. These deviations from the mean are common to the facility, as fuel is supplied in pulses from overhead the combustion chamber, thus introducing cool batches of fuel

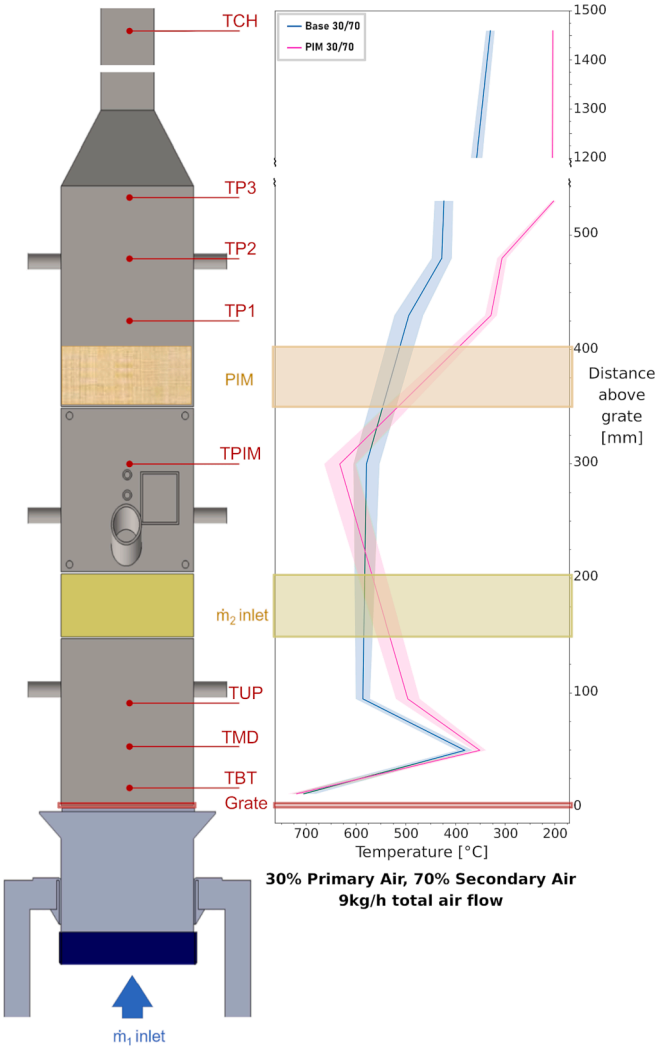

Fig. 5. Temperature evolution of 30/70 tests.

inside the reacting combustion chamber, slightly altering its behavior, and reducing temperature overall. Gas leaves the controlled area at temperatures around 400 °C.

The tests that included a PIM show significantly different profiles. While the maximum temperatures are still located in the combustion chamber, local maxima are detected in the thermocouple located directly underneath the PIM, with values closely resembling those of the combustion bed area suggesting the possibility of reactions occurring in the area at a similar pace as at the bed. After the PIM, a sharp decline in temperature ensues, with a ΔT of 300 °C in the space of 100 mm, sinking the values below the minima detected in Base tests. Another clear consequence of the placing of PIM is the stabilization of readings, with instabilities being reduced significantly, due to the lamination of the flow caused by the PIM acting as a filter, behavior that was also detected in our previous research on PIM combustion [37]. Table 2 shows the temperatures that best represent this behavior and their deviation from the mean, that results clearly inferior in the PIM tests.

The second batch of tests delivered similar results, as seen in Fig. 6. 50 % primary air and 50 % secondary it is a common reference framework for the facilities in our research group. Worse behavior relative to plant stability and emissions are expected, and the results are in line with what was foreseen. A higher primary air proportion caused higher activation of the bed reactions and so, higher temperatures in the fireplace with an associated increase in standard deviation either in baseline and PIM cases. The greater difference between the two setups is the location of the peak temperature and its distribution. For Base tests, temperature stays around the 600 °C mark for the first half of the measurement area, up until the inlet of secondary air, then dropping to 400 °C and exiting the facility.

PIM tests show a clear difference in line with the results of the previous batch, although peak temperature is located outside the combustion chamber, immediately below the secondary air inlet and the PIM itself. This could be due to the higher velocity of gas, that drags reacting components away from the lower levels of the combustion chamber and into the heat-confinement area below the PIM, where enough heat concentrates to create optimal conditions for reaction. After the PIM a heavy drop in temperature is noticeable, with a ΔT of 350 °C in the space of 100 mm and, similarly to the base tests, temperatures in the outlet regions stay around 200 °C. Minimal variability of temperature measurement is achieved at the outlet in PIM tests, but the standard deviation is remarkably lower than base tests in all thermocouples. These comparisons can be seen in Table 4.

The higher temperatures detected in all cases where the PIM was present corresponded with higher temperatures in the cooling water flowing through some sections of the facility, such as the lower part of the chimney. These increases were most notable in 30/70 tests, where temperatures in the outlet water were a 30–40 % higher than in base tests, while increases of a 15 % were detected in the 50/50 tests. The observed behavior fits reasonably well with previous experiences, where it was shown that the effect of the PIM is an optical barrier that manages to increase the temperature of the lower gas zone [37]. Unfortunately, from the point of view of gaseous emissions (once we put them together in this section) the turbulence is affected, slightly increasing the emission of unburned and NOx.

3.1.1. Gaseous emissions

Gaseous emission data is presented in Fig. 8. The effect of the PIM stands clear in the case of CO emission, where a substantial increase is detected. This increase could be attributed to the reactions between oxidizer and carbon not having enough residence time to complete, as the temperatures past the PIM are too low to continue the reaction. This result corroborated our previous experiences, as a PIM located too close to the flame and secondary air inlet proved in the past to be responsible for an increased proportion of incomplete combustion products [37]. Nitrogen oxides remain in similar values for 50/50 tests, but also experiment an increase in 30/70 tests with and without PIM. The main

Table 3
Selected temperatures of 30/70 tests.

Base 30/70			PIM 30/70		
Distance above grate (mm)	Temperature (°C)	standard deviation	**Distance above grate (mm)**	Temperature (°C)	Standard deviation
12	704.50	23.67	**12**	719.08	16.60
300	578.63	26.30	**300**	632.25	11.82
530	422.83	18.63	**530**	202.10	4.40

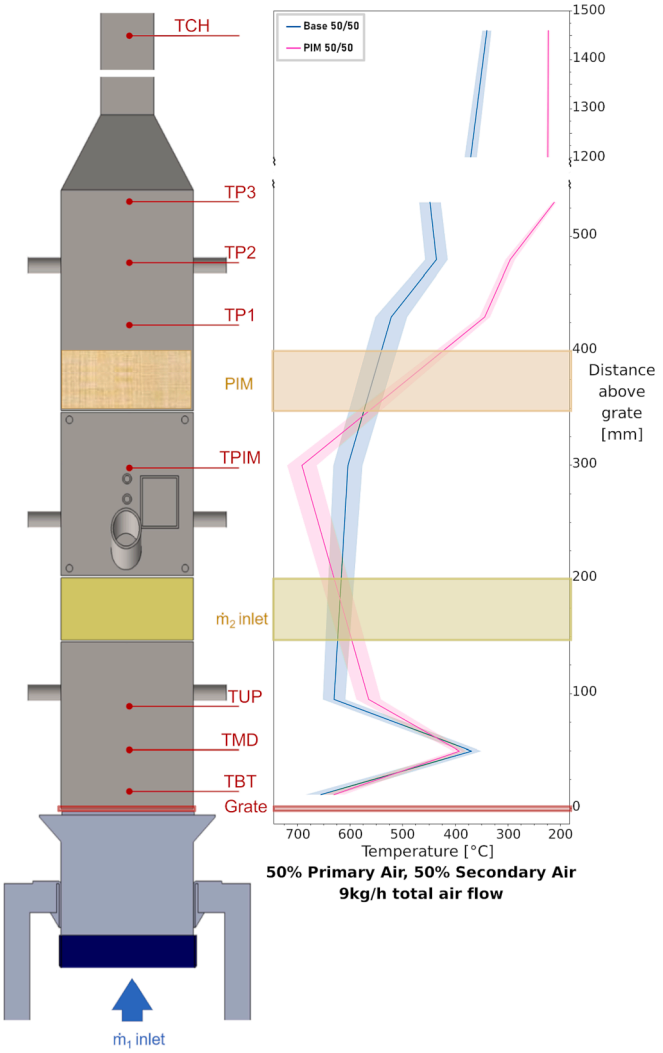

Fig. 6. Temperature evolution of 50/50 tests.

conclusion obtained is, once more, the stabilization of measurements, especially noticeable in 30/70 tests for NOx, as the measurements in a no-PIM scenario have a high standard deviation that gets reduced substantially with the placement of the PIM.

3.2. PM emissions

3.2.1. PM during VOC sampling

The sample of PM taken while sampling VOC was obtained by forcing the extracted gas through a PTFE filter. This filter has a mesh size of 0.3 μm, and thus is not able to properly gather data on finer PM. The results of this sampling are gathered in Fig. 7, where the greyed area represents the PM that the PTFE filter can capture. From the bar graph it is evident that PM is reduced in the 30/70 scenarios due to the effect of the PIM, and the elimination of instabilities in measurements that was mentioned previously is very clear here, with repeated measurements that diverge a mere 4 %. The results presented here for this configuration coincide with those observed in previous research on PIM inside laboratory combustors, with clear reductions in the amount of PIM sampled in the exhaust gas, being the air-staging strategy the key factor in this reduction [37,38]. In the current scenario, the same air-staging used in previous research has proven once more to be the most favorable scenario for the use of PIM.

For 50/50 tests, the difference between PIM and Base scenarios is not clear, with similar averages and overlapping standard deviations. This could be attributed to the reaction zone being displaced towards the lower parts of the combustion chamber, as a higher proportion of oxidizer is present there, and temperatures are also high enough to guarantee the activation energy required for the reaction to take place. This displacement of the reaction area minimizes the effect of the heat confinement caused by the PIM, as fewer amounts of unreacted matter reach the PIM. This, added to the lower proportion of air entering through the adjacent secondary air inlet, results in a poorer mixture over which the PIM is unable to offer any advantages in the reduction of PM.

Overall, the data suggests that the reduction of PIM is primarily of that solid matter with the biggest aerodynamic diameter, 0.3 μm and higher, and that this reduction is most effective when the proportion of air in the primary inlet is low. This allows for a better outcome from the secondary reaction zone, resulting in an overall lower PM emission.

3.3. VOC data

3.3.1. Emissions

VOC emissions followed a similar tendency to PM emissions, as can be observed in Fig. 8. The base scenarios show similar values and standard deviations for both air-staging strategies, while the PIM tests behave very dissimilarly. The increase in in-chamber temperature detected in 30/70 PIM compared to the base scenario is assumed to be responsible for the decrease of VOC capture, as a higher temperature would facilitate reaction and decomposition of substances as soon as they are generated in the combustion reaction. In 50/50 tests this temperature actually decreases from base to PIM tests, which could in itself explain the higher quantity of VOCs detected. This also highlights

Table 4
Selected temperatures of 50/50 tests.

Base 50/50			PIM 50/50		
Distance above grate (mm)	Temperature (°C)	Standard deviation	**Distance above grate (mm)**	Temperature (°C)	Standard deviation
12	654.82	28.23	**12**	629.85	19.16
300	603.65	27.57	**300**	691.06	27.98
530	447.69	20.42	**530**	211.79	3.72

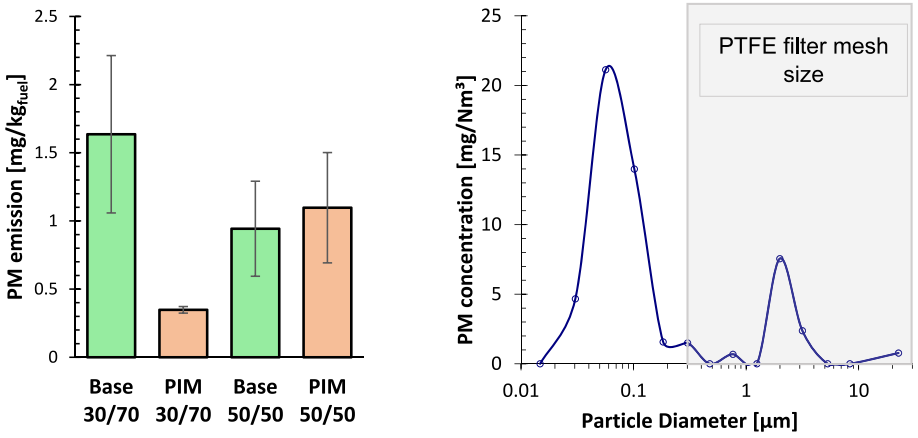

Fig. 7. PM emissions captured by PTFE filter (left) and visualization of sizes covered (right).

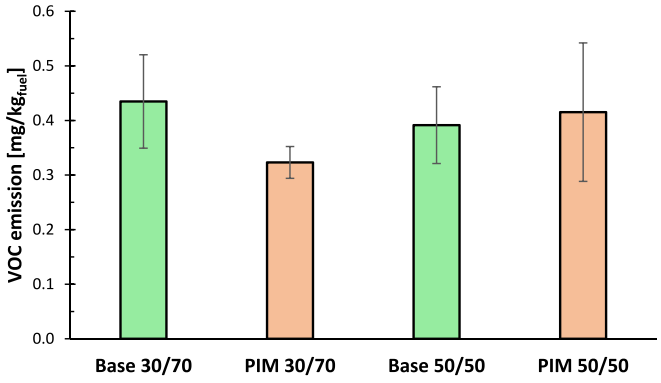

Fig. 8. VOCs detected by the impinger train.

the relative relevance of higher temperatures in the immediate surroundings of the fuel compared to temperatures around the secondary air inlet. This could be attributed to the higher concentration of VOCs in the area of their generation, making reactions more feasible than in the more diluted upstream sections.

The influence of PIM in measurement reliability can also be noticed, with a stark contrast between 30/70 and 50/50 air-staging strategies. 30/70 tests show a decrease in the overall variation of the measurements when a PIM is present, due to the lamination of the fluid effect that was already mentioned in previous sections. On 50/50 tests, this effect is not present, with a larger standard deviation in PIM tests than in base scenarios. This could be caused by the effect of such large proportion of primary air, which is causing a great disturbance in the gas flow leading to the instabilities shown.

3.3.2. *Sample degradation*

A portion of used AC is subjected to the thermal treatment described previously, consisting in a stepping climb from ambient temperature to 120 °C to understand the evolution of the adsorbed compounds in time. Each time a portion was taken out of the sample, the rest of it is stored back inside a zip bag in a glass desiccator until the next TGA was due. The results of these analyses are shown in Fig. 9, and they reveal the high affinity of AC for lighter organic substances in detriment of the retention of heavier ones. The results are shown as percentage of total mass loss of the sample introduced in the TGA devices, as the mass of the adsorbed substances represents only a small fraction of the total mass of AC.

It can be noted that AC examined right after sample collection in the combustion facility experiments a mass loss during the entire cycle that can be subdivided into two trends. The first part of the mass loss curve (from 20 to 40 °C) shows the desorption of lighter organic substances, such as phenols and other simple benzene-derived compounds. These are known to be substances towards which AC has a high affinity, and as such their presence is expected in the sample. The second part (40 to 120 °C) corresponds to heavier compounds, that require more energy to be desorbed from the AC matrix. This area is characterized for a slower decline, given that the mass of these heavier VOCs retained is not as significant, and the variety of compounds that fit in this category is

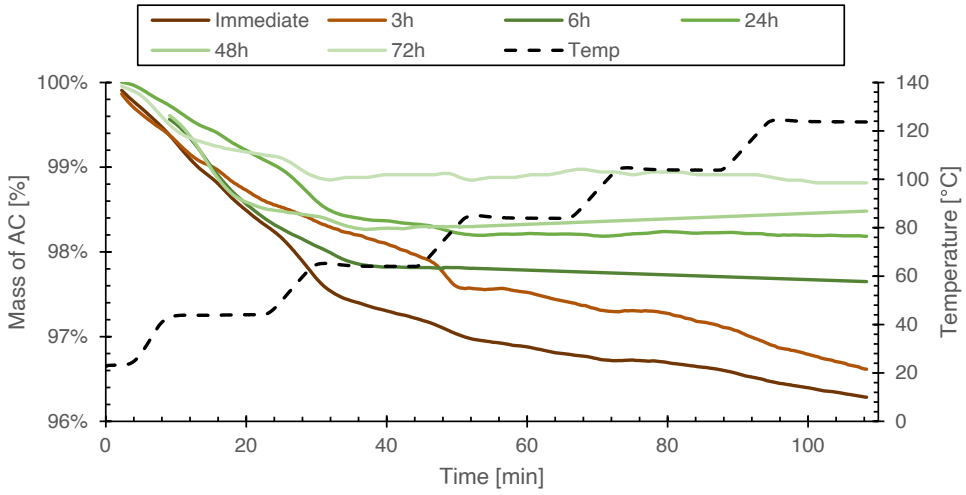

Fig. 9. TGA of the degradation of the samples.

substantial.

The first result that is revealed from the data is that the second area of desorption is only present at the samples analyzed immediately and three hours after VOC capture, all but disappearing afterwards. This could indicate that affinity between the molecules and AC is not enough to ensure a sustained adsorption of these substances, and thus the time factor becomes a critical part of measurement and analysis. The selectivity of AC for certain volatiles such as BTEX or chlorinated hydrocarbons has been reported in previous literature, where recovery ratios of these substances nearing 100 % have been attested [51–53]. Besides, the temperature at which the capture is made is below the analysis temperature, a factor that also could hamper the retention of very volatile substances. For samples analyzed 6 h from the adsorption and onwards, the first desorption area is clearly still present, and desorption of substances stops at 60 °C in every case after the 3-hour mark. A clear tendency to the loss of sample is also detected, with AC desorbing less mass the more time has passed from the adsorption event. It is estimated that after 4 to 5 days from the adsorption, the amount of VOC still contained in the AC would be insignificant, even with the measures in place to prevent the contact of AC with the atmosphere.

4. Conclusions

The data presented indicates that the inclusion of a PIM, when successful in retaining heat in the lower combustion chamber, is a useful strategy to reduce the VOC emissions detectable by the active carbon, with reductions numbering up to a 20 % in best case scenarios. These best case scenarios were found to be the tests with a 30/70 air staging ratio, where the PIM caused the emission of VOC to diminish from 0.42 mg/kg_{fuel} to 0.33 mg/kg_{fuel} on average. The sampling train proposed was successful in the capture of a fraction of the volatile chemicals, especially the lightest compounds as shown by the desorption temperatures detected in the TGA tests. The study on sample preservation time revealed that adsorbed substances are released quickly after their capture, even when stored inside sealed containers and in a controlled environment. The optimal measurement time is under 6 h, time at which a sharp decline in substances adsorbed is detected, and this should be taken into consideration for in-site, out-of-laboratory measurements. The results presented open new paths for the development of VOC capture, containment, and reduction systems. As the time factor has proven to be essential in the correct determination of VOC presence in a gas current, systems such as the one designed for the purpose of this research are of utmost relevance for both scientists and industries. The future of in situ measurement and analysis of VOC relies on portable, sturdy, and reliable devices that are capable of performing accurate measurements. Meanwhile, this research has also confirmed the ability of PIM systems for the reduction of both PM and VOC pollution.

CRediT authorship contribution statement

Juan Jesús Rico: Conceptualization, Data curation, Formal analysis, Investigation, Methodology, Software, Validation, Writing – original draft, Writing – review & editing. **Raquel Pérez-Orozco:** Conceptualization, Data curation, Methodology, Visualization, Writing – review & editing. **Jacobo Porteiro:** Project administration, Resources, Supervision, Writing – review & editing. **David Patiño:** Funding acquisition, Project administration, Resources, Supervision.

Declaration of Competing Interest

The authors declare that they have no known competing financial interests or personal relationships that could have appeared to influence the work reported in this paper.

Data availability

Data will be made available on request.

Acknowledgement

This research was financially supported by the project PID2021-126569OB-I00 of the Ministry of Science and Innovation (Spain) and the AVIENERGY project, jointly financed by the European Agricultural Fund for Rural Development (EAFRD) on an 80% and by the Ministerio de Agricultura, Pesca y Alimentación on a 20%. Funding for open access charge: Universidade de Vigo/CISUG. The work of Juan Jesús Rico Fuentes was supported by a grant from the University of Vigo.

Appendix A. Supplementary data

Supplementary data to this article can be found online at https://doi.org/10.1016/j.fuel.2023.128907.

References

[1] Trypolska G, Rosner A. The use of solar energy by households and energy cooperatives in post-war Ukraine: lessons learned from Austria. Energies 2022;15:7610. https://doi.org/10.3390/en15207610.
[2] Yakymchuk A, Kardash O, Popadynets N, Yakubiv V, Maksymiv Y, Hryhoruk I, et al. Modeling and governance of the country's energy security: the example of Ukraine. Int J Energy Econ Policy 2022;12:280–6. https://doi.org/10.32479/ijeep.13397.
[3] Jiang P, Fan YV, Klemeš JJ. Impacts of COVID-19 on energy demand and consumption: challenges, lessons and emerging opportunities. Appl Energy 2021;285:116441. https://doi.org/10.1016/j.apenergy.2021.116441.
[4] Kuzemko C, Bradshaw M, Bridge G, Goldthau A, Jewell J, Overland I, et al. Covid-19 and the politics of sustainable energy transitions. Energy Res Soc Sci 2020;68:101685. https://doi.org/10.1016/j.erss.2020.101685.
[5] Mofijur M, Fattah IMR, Alam MA, Islam ABMS, Ong HC, Rahman SMA, et al. Impact of COVID-19 on the social, economic, environmental and energy domains: lessons learnt from a global pandemic. Sustain Prod Consum 2021;26:343–59. https://doi.org/10.1016/j.spc.2020.10.016.
[6] Kornhuber K, Osprey S, Coumou D, Petri S, Petoukhov V, Rahmstorf S, et al. Extreme weather events in early summer 2018 connected by a recurrent hemispheric wave-7 pattern. Environ Res Lett 2019;14(5):054002. https://doi.org/10.1088/1748-9326/ab13bf.
[7] Jufri FH, Widiputra V, Jung J. State-of-the-art review on power grid resilience to extreme weather events: definitions, frameworks, quantitative assessment methodologies, and enhancement strategies. Appl Energy 2019;239:1049–65. https://doi.org/10.1016/j.apenergy.2019.02.017.
[8] Jain P, Wang X, Flannigan MD. Trend analysis of fire season length and extreme fire weather in North America between 1979 and 2015. Int J Wildland Fire 2017;26:1009. https://doi.org/10.1071/WF17008.
[9] Koppmann R, editor. Volatile organic compounds in the atmosphere. Oxford, UK: Blackwell Publishing Ltd; 2007. https://doi.org/10.1002/9780470988657.
[10] Ciccioli P, Brancaleoni E, Frattoni M, Cecinato A, Pinciarelli L. Determination of volatile organic compounds (VOC) emitted from biomass burning of Mediterranean vegetation species by GC-MS. Anal Lett 2001;34:937–55. https://doi.org/10.1081/AL-100103604.
[11] Tan Z, Lu K, Dong H, Hu M, Li X, Liu Y, et al. Explicit diagnosis of the local ozone production rate and the ozone-NOx-VOC sensitivities. Sci Bull 2018;63(16):1067–76. https://doi.org/10.1016/j.scib.2018.07.001.
[12] Jin X, Fiore A, Boersma KF, Smedt ID, Valin L. Inferring changes in summertime surface ozone–NO_x–VOC chemistry over U.S. Urban areas from two decades of satellite and ground-based observations. Environ Sci Technol 2020;54:6518–29. https://doi.org/10.1021/acs.est.9b07785.
[13] Davardoost F, Kahforoushan D. Health risk assessment of VOC emissions in laboratory rooms via a modeling approach. Environ Sci Pollut Res 2018;25:17890–900. https://doi.org/10.1007/s11356-018-1982-6.
[14] Dai H, Jing S, Wang H, Ma Y, Li L, Song W, et al. VOC characteristics and inhalation health risks in newly renovated residences in Shanghai, China. Sci Total Environ 2017;577:73–83. https://doi.org/10.1016/j.scitotenv.2016.10.071.
[15] Mo Z, Lu S, Shao M. Volatile organic compound (VOC) emissions and health risk assessment in paint and coatings industry in the Yangtze River Delta. China Environ Pollut 2021;269:115740. https://doi.org/10.1016/j.envpol.2020.115740.
[16] Sarkar C, Sinha V, Sinha B, Panday A, Rupakheti M, Lawrence M. Source apportionment of NMVOCs in the Kathmandu Valley during the SusKat-ABC international field campaign using positive matrix factorization. Atmospheric Chem Phys 2017;17:8129–56. https://doi.org/10.5194/acp-17-8129-2017.
[17] Baudic A, Gros V, Sauvage S, Locoge N, Sanchez O, Sarda-Estève R, et al. Seasonal variability and source apportionment of volatile organic compounds (VOCs) in the Paris megacity (France). Atmospheric Chem Phys 2016;16(18):11961–89. https://doi.org/10.5194/acp-16-11961-2016.

[18] Yadav R, Sahu LK, Tripathi N, Pal D, Beig G, Jaaffrey SNA. Investigation of emission characteristics of NMVOCs over urban site of western India. Environ Pollut 2019;252:245–55. https://doi.org/10.1016/j.envpol.2019.05.089.

[19] Cai M, An C, Guy C. A scientometric analysis and review of biogenic volatile organic compound emissions: research hotspots, new frontiers, and environmental implications. Renew Sustain Energy Rev 2021;149:111317. https://doi.org/10.1016/j.rser.2021.111317.

[20] Song S-K, Shon Z-H, Kang Y-H, Kim K-H, Han S-B, Kang M, et al. Source apportionment of VOCs and their impact on air quality and health in the megacity of Seoul. Environ Pollut 2019;247:763–74. https://doi.org/10.1016/j.envpol.2019.01.102.

[21] Chen C-C, Huang Y-H, Hung S-M, Chen C, Lin C-W, Yang H-H. Hydrophobic deep eutectic solvents as attractive media for low-concentration hydrophobic VOC capture. Chem Eng J 2021;424:130420. https://doi.org/10.1016/j.cej.2021.130420.

[22] Rodriguez Castillo A-S, Biard P-F, Guihéneuf S, Paquin L, Amrane A, Couvert A. Assessment of VOC absorption in hydrophobic ionic liquids: Measurement of partition and diffusion coefficients and simulation of a packed column. Chem Eng J 2019;360:1416–26. https://doi.org/10.1016/j.cej.2018.10.146.

[23] Yang Fu, Lu Y, Li W, Tu W, Li L, Wang X, et al. Route-optimized synthesis of bagasse-derived hierarchical activated carbon for maximizing volatile organic compound (VOC) adsorption capture properties. ChemistrySelect 2021;6(38):10362–8. https://doi.org/10.1002/slct.202101295.

[24] Maximoff SN, Mittal R, Kaushik A, Dhau JS. Performance evaluation of activated carbon sorbents for indoor air purification during normal and wildfire events. Chemosphere 2022;304:135314. https://doi.org/10.1016/j.chemosphere.2022.135314.

[25] Yun J-H, Hwang K-Y, Choi D-K. Adsorption of benzene and toluene vapors on activated carbon fiber at 298, 323, and 348 K. J Chem Eng Data 1998;43:843–5. https://doi.org/10.1021/je980069a.

[26] Li L, Liu S, Liu J. Surface modification of coconut shell based activated carbon for the improvement of hydrophobic VOC removal. J Hazard Mater 2011;192:683–90. https://doi.org/10.1016/j.jhazmat.2011.05.069.

[27] Ouzzine M, Romero-Anaya AJ, Lillo-Ródenas MA, Linares-Solano A. Spherical activated carbons for the adsorption of a real multicomponent VOC mixture. Carbon 2019;148:214–23. https://doi.org/10.1016/j.carbon.2019.03.075.

[28] Bravo I, Figueroa F, Swasy MI, Attia MF, Ateia M, Encalada D, et al. Cellulose particles capture aldehyde VOC pollutants. RSC Adv 2020;10(13):7967–75. https://doi.org/10.1039/D0RA00414F.

[29] Dwivedi P, Gaur V, Sharma A, Verma N. Comparative study of removal of volatile organic compounds by cryogenic condensation and adsorption by activated carbon fiber. Sep Purif Technol 2004;39:23–37. https://doi.org/10.1016/j.seppur.2003.12.016.

[30] Swasy MI, Campbell ML, Brummel BR, Guerra FD, Attia MF, Smith GD, et al. Poly (amine) modified kaolinite clay for VOC capture. Chemosphere 2018;213:19–24. https://doi.org/10.1016/j.chemosphere.2018.08.156.

[31] An Y, Fu Q, Zhang D, Wang Y, Tang Z. Performance evaluation of activated carbon with different pore sizes and functional groups for VOC adsorption by molecular simulation. Chemosphere 2019;227:9–16.

[32] Pérez-Orozco R, Patiño D, Porteiro J, Rico JJ. The effect of primary measures for controlling biomass bed temperature on PM emission through analysis of the generated residues. Fuel 2020;280:118702. https://doi.org/10.1016/j.fuel.2020.118702.

[33] Khodaei H, Guzzomi F, Yeoh GH, Regueiro A, Patiño D. An experimental study into the effect of air staging distribution and position on emissions in a laboratory scale biomass combustor. Energy 2017;118:1243–55. https://doi.org/10.1016/j.energy.2016.11.008.

[34] Regueiro A, Patiño D, Porteiro J, Granada E, Míguez JL. Effect of air staging ratios on the burning rate and emissions in an underfeed fixed-bed biomass combustor. Energies 2016;9. https://doi.org/10.3390/en9110940.

[35] Rico JJ, Pérez-Orozco R, Cid N, Larrañaga A, Tabarés JLM. Viability of agricultural and forestry residues as biomass fuels in the galicia-north portugal region: an experimental study. Sustain Switz 2020;12. https://doi.org/10.3390/su12198206.

[36] Liu H, Chaney J, Li J, Sun C. Control of NOx emissions of a domestic/small-scale biomass pellet boiler by air staging. Fuel 2013;103:792–8. https://doi.org/10.1016/j.fuel.2012.10.028.

[37] Rico JJ, Patiño D, Cid N, Pérez-Orozco R. PM reduction and flame confinement in biomass combustion using a porous inert material. Fuel 2020;280. https://doi.org/10.1016/j.fuel.2020.118496.

[38] Guerrero F, Arriagada A, Muñoz F, Silva P, Ripoll N, Toledo M. Particulate matter emissions reduction from residential wood stove using inert porous material inside its combustion chamber. Fuel 2021;289:119756. https://doi.org/10.1016/j.fuel.2020.119756.

[39] Ciria D, Orihuela MP, Becerra JA, Chacartegui R, Ramírez-Rico J. Impact of flame confinement with inert ceramic foams on the particulate emissions of domestic heating systems. Fuel 2021;304:121264. https://doi.org/10.1016/j.fuel.2021.121264.

[40] Pérez-Orozco R, Patiño D, Porteiro J, Larrañaga A. Flue gas recirculation during biomass combustion: implications on PM release. Energy Fuels 2020;34:11112–22. https://doi.org/10.1021/acs.energyfuels.0c02086.

[41] Cid N, Patiño D, Pérez-Orozco R, Porteiro J. Performance analysis of a small-scale electrostatic precipitator with biomass combustion. Biomass Bioenergy 2022;162:106500. https://doi.org/10.1016/j.biombioe.2022.106500.

[42] Regueiro A, Jezerská L, Patiño D, Pérez-Orozco R, Nečas J, Žídek M. Experimental study of the viability of low-grade biofuels in small-scale appliances. Sustain Switz 2017;9. https://doi.org/10.3390/su9101823.

[43] Marcotte S, Castilla C, Morin C, Merlet-Machour N, Carrasco-Cabrera L, Medaerts F, et al. Particulate inorganic salts and trace element emissions of a domestic boiler fed with five commercial brands of wood pellets. Environ Sci Pollut Res 2020;27(15):18221–31. https://doi.org/10.1007/s11356-020-08329-8.

[44] Brachi P, Chirone R, Miccio M, Ruoppolo G. Fluidized bed torrefaction of commercial wood pellets: process performance and solid product quality. Energy Fuels 2018;32:9459–69. https://doi.org/10.1021/acs.energyfuels.8b01519.

[45] Manić N, Janković B, Milović L, Komatina M, Stojiljković D. The impact of production operating parameters on mechanical and thermophysical characteristics of commercial wood pellets. Biomass Convers Biorefinery 2023;13(7):5787–803. https://doi.org/10.1007/s13399-021-01609-4.

[46] Pérez-Orozco R, Patiño D, Porteiro J, Míguez JL. Novel test bench for the active reduction of biomass particulate matter emissions. Sustain Switz 2020;12. https://doi.org/10.3390/SU12010422.

[47] Pérez-Orozco R, Patiño D, Porteiro J, Míguez JL. Bed cooling effects in solid particulate matter emissions during biomass combustion. A morphological insight. Energy 2020;205:118088. https://doi.org/10.1016/j.energy.2020.118088.

[48] Wang H, Xu J, Liu X, Sheng L. Preparation of straw activated carbon and its application in wastewater treatment: a review. J Clean Prod 2021;283:124671. https://doi.org/10.1016/j.jclepro.2020.124671.

[49] Wang Y-H, Bayatpour S, Qian X, Frigo-Vaz B, Wang P. Activated carbon fibers via reductive carbonization of cellulosic biomass for adsorption of nonpolar volatile organic compounds. Colloids Surf Physicochem Eng Asp 2021;612:125908. https://doi.org/10.1016/j.colsurfa.2020.125908.

[50] Rahbar-Shamskar K, Aberoomand Azar P, Rashidi A, Baniyaghoob S, Yousefi M. Synthesis of micro/mesoporous carbon adsorbents by in-situ fast pyrolysis of reed for recovering gasoline vapor. J Clean Prod 2020;259:120832. https://doi.org/10.1016/j.jclepro.2020.120832.

[51] Chary NS, Fernandez-Alba AR. Determination of volatile organic compounds in drinking and environmental waters. TrAC Trends Anal Chem 2012;32:60–75. https://doi.org/10.1016/j.trac.2011.08.011.

[52] Sun T, Jia J, Fang N, Wang Y. Application of novel activated carbon fiber solid-phase, microextraction to the analysis of chlorinated hydrocarbons in water by gas chromatography–mass spectrometry. Anal Chim Acta 2005;530:33–40. https://doi.org/10.1016/j.aca.2004.08.042.

[53] Martí I, Lloret R, Martín-Alonso J, Ventura F. Determination of chlorinated toluenes in raw and treated water samples from the Llobregat river by closed loop stripping analysis and gas chromatography–mass spectrometry detection. J Chromatogr A 2005;1077:68–73. https://doi.org/10.1016/j.chroma.2005.04.051.